International Journal of Thermal Sciences 48 (2009) 2139–2147

Contents lists available at ScienceDirect

International Journal of Thermal Sciences

journal homepage: www.elsevier.com/locate/ijts

Thermal characteristics of tree-shaped microchannel nets with/without loops

Peng Xu [a,b], X.Q. Wang [a], A.S. Mujumdar [a,*], C. Yap [a], B.M. Yu [b]

[a] Department of Mechanical Engineering, National University of Singapore, Singapore 117576
[b] School of Physics, Huazhong University of Science and Technology, Wuhan 430074, P.R. China

ARTICLE INFO

Article history:
Received 27 November 2008
Received in revised form
27 March 2009
Accepted 27 March 2009
Available online 6 May 2009

Keywords:
Tree-shaped net
Loop
Pressure drop
Blockage
Electronic component cooling

ABSTRACT

Several tree-shaped microchannel networks with/without loops are numerically examined and compared for application in cooling of electronic components. The physical model of microchannel electronic cooling system is set up with tree-shaped networks. The tree-shaped microchannel nets are embedded in a disk-shaped heat sink, which is attached to a chip to remove the heat dissipated by a chip. The effects of total branching level and loops on the thermal and flow performances of heat sink system are investigated numerically. Results show that tree-shaped nets with loops provide a great advantage when the structure experiences accidental damage to one or more channel segments since the loop assures continuity of coolant flow. Under blockage of some branches, the channel networks only experience an increase of pressure drop while maintaining the capability to remove the heat generated by the chip.

1. Introduction

The efficient transport characteristics of natural tree-shaped systems such as trees, leaves, mammalian circulatory and respiratory systems, vascular tissues, neural dendrites, river basins, oil/water reservoir, street, etc. can shed light on optimal solutions of many practical problems, which have fascinated researchers in physics, chemistry, biology, physiology, engineering and geology for ages. The transport properties of the tree-shaped systems have been broadly investigated [1–5]. Recently, the constructal principle maximizing global performance in a constrained but morphing flow structure was presented as a mechanism of optimizing and designing by Bejan [1]. The constructal theory was first proposed in a problem of pure heat conduction [6], and was extended to design the structure of convective fins [7], fluid flow [8,9], and heat transfer [10,11]. Recently, it has been widely applied in design of photovoltaic cells [12], thermochemical reactor [13], prediction of droplet impact geometry and particle agglomeration [14,15], optimization of heat sinks [16], self-healing smart materials [17,18], and even green energy as well as global circulation and climate [19,20], and so on. Optimized pipe connections (topology) can be found following the constructal theory and exhibit tree-shaped branching structures [1].

The performance of tree-shaped nets can be enhanced but at the cost of increased complexity of geometry. However, the increased geometric complexity involves problems in manufacture so that we need to reduce complexity in design. Also, as discussed by Wang et al. [10], the increased complexity of the net geometries does not necessarily improve their performance. Hence, it is necessary to seek other effective ways, other than increasing the geometric complexity, to optimize tree-shaped nets, especially if potentially blockage of flow may occur in any of the channel segments, which can affect the cooling performance adversely.

Point-circle tree-shaped networks have been already recognized as useful designs for electronics cooling [21], which will be taken in the current study to investigate the heat transfer in heat sink system. If we examine the design of most leaves, we find that the channel nets have a "tree-shape" with many small loops between channel segments. With such a structure, the loops are served by the peripheral duct flow even with blockage of some channel segments. Inclusion of loops can enhance performance reliability and stability of the cooling systems while maintaining a relatively simple design of the geometry. Wechsatol et al. analytically examined the fundamental attributes of constructal networks with loops, and indicated that incorporating loop is an effective design strategy to maintain a high level of global performance reliability when the networks experience local blockage [22]. Rocha et al. discussed the cooling performance of tree architectures with loops and found that trees with two loop sizes are marginally inferior to trees with only one loop size, although the robustness of tree-with-loops architectures

* Corresponding author. Tel.: +65 6874 4623; fax: +65 6779 1459.
E-mail address: mpeasm@nus.edu.sg (A.S. Mujumdar).

1290-0729/$ – see front matter © 2009 Elsevier Masson SAS. All rights reserved.
doi:10.1016/j.ijthermalsci.2009.03.018

Nomenclature

A	surface area of the network, mm^2
c_p	specific heat capacity, J/kg K
d	hydraulic diameter of channel segment, mm
f	friction factor
h	height, mm
l	channel segment length, mm
m	total number of branching levels
$\dot{m}$	mass flow, g/s
n	number of bifurcation per channel
N	number of channels emanating from the center of the disc
p	pressure, Pa
q''_0	hear flux, W/m^2
r	radius of disc, mm
Re	Reynolds number
T	temperature, K
ΔT	temperature difference, K
V	velocity, m/s
w	width of channel segment, mm
w'	width of loop, mm
X	dimensionless x coordinate, $X = x/r$
x, y, z	Cartesian coordinate, mm

Greek symbols

λ	thermal conductivity, W/m K
μ	dynamic viscosity, Pa s
ρ	density, kg/m^3
θ	branching angle

Subscripts

c	chip
t	tree-shaped microchannel net
i,j	indices in Einstein summation convention, sequence number
k	branching level, 0,1,2,…
max	maximum
s	heat sink

increases [23]. However, only conduction was considered in their analysis. Wang et al. also discussed the effect of *single* level loops in tree-shaped nets on the flow and thermal performance [11]. They found that the inclusion of loops between the outlets in the constructal nets provides a significant advantage when the structure experiences accidental damage to one or more of its sub-channel segments since the loop assures continuity of flow. In spite of blockage, the performance of network suffers only a small performance drop while experiencing increased pressure drop.

This study attempts to obtain further understanding of the key features of tree-shaped nets with *multiple* loops by Computational Fluid Dynamics (CFD) in three dimensions in conjunction with a constant heat flux boundary condition at the channel walls. The effect of branching level (geometrical complexity) of tree-shaped nets on the thermal characteristics has been calculated numerically. Comparison between tree-shaped nets with loops and those without loops, nets without blockage and those with blockage has been carried out to explore the problems.

2. Model and analysis

Consider a typical configuration, which is a three-dimensional heat sink with embedded looped tree-shaped microchannel networks as shown in Fig. 1. The physical model include three parts: heat sink (in silicon) at the top, tree-shaped micochannel networks embedded in the heat sink (black shaded part) and the chip at the bottom attached to the heat sink. The heat generated by the chip can be removed by the tree-shaped micochannel networks in the system. Note that the loops can be activated or de-activated for the purpose of comparison.

For the generation of tree-shaped networks, the optimal construct for fluid flow will be adopted. Although Murray's law was presented from blood vessels [24], it has been shown to be suitable for many other biology tissues, even for no-living systems [25]. According to Murray's law, the cube of the radius of a parent vessel should equal to the sum of the cubes of the radii of the daughter vessels such that the global flow resistance is minimized. Based on the suggestion made by West et al. for two-dimensional flow networks [26], Pence [21] developed a preliminary symmetrical

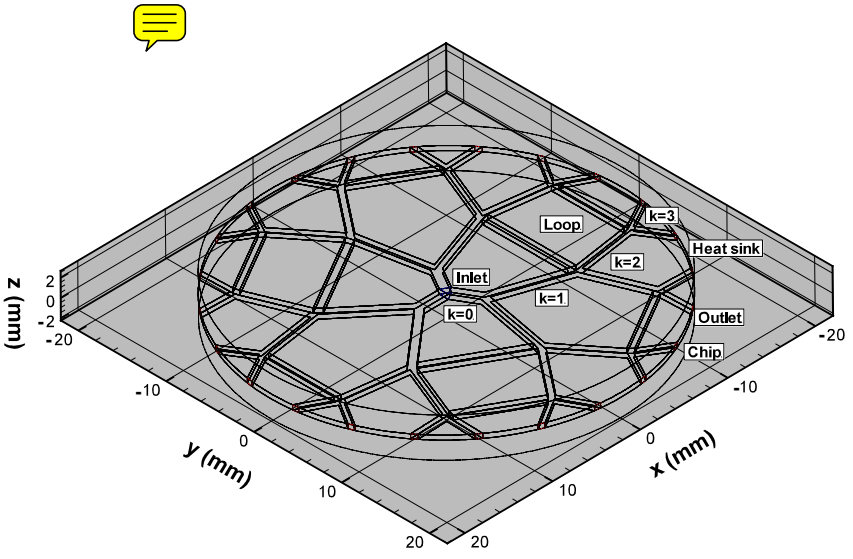

Fig. 1. Typical physical model of heat sink system embedded in tree-shaped microchannel nets ($n = 2$, $m = 3$).

branching channel network in a disk-shaped heat sink using the following diameter branching ratios,

$$d_{k+1}/d_k = n^{-1/3} \quad (1)$$

Note in Fig. 1 that the three first branches emanating from the inlet flow plenum are the zeroth-order branch, i.e., $k=0$, branching number $n=2$ and the total number of branching levels is $m=3$. However, it was noted by Pence and Enfield that there is a major problem in going high branching levels when using conventional hydraulic diameter to define the branching ratio to characterize rectangular channels for fixed channel height [27]. Hence, based on their suggestion, a fixed width ratio was employed in this study.

$$w_{k+1}/w_k = n^{-1/3} \quad (2)$$

For the length of tree-shaped nets, there is no such fixed law as Murray's law to determine the length branching ratio. However, the optimal length ratio can be obtained with some extra constrains. For example, Bejan et al. derived the optimal length branching ratio which is the same as diameter branching ratio via minimizing the flow resistance under fixed volume and area for T-shaped single branch [28]. Thus, the length of microchannels can be determined according to the space constrains in the current simulations. For the symmetrical branch, the optimal branching angle is $\theta = 74.94^\circ$ [29]. However, the branching angle need to be adjusted at each level in disc-shaped heat sink systems to make sure that the end of all the last branches reaches the boundary of disc-shaped heat sink system uniformly.

A two-dimensional view of such a flow network is shown in Fig. 2. For the present analysis, the radius of heat sink systems $r=20$ mm, branching number $n=2$. In the current study, four cases $m=1$, $m=2$, $m=3$ and $m=4$ are simulated. Accordingly, the hydraulic diameter and width are determined by Eqs. (1) and (2), while the channel length l and branching angle θ vary with total number of branching level m. For the dimensions of the loops, to simplify the problem, the width w'_k is kept constant and equal to the corresponding channel width w_k. Accordingly, the surface area of the tree-shaped network A will be different for different branching level m. Dimensions of the flow network are listed in Table 1. The inlet cross-section area is held fixed for consistent comparison with previous studies in which the total convective area was held constant [30]. The reason for this choice is that when the inlet cross-section area is fixed, the inlet mass flow and Reynolds number are constant for all comparable cases, although the total convection area would increase with increased number of branch levels, as seen in Table 1. Note that in Fig. 2 the sub-channels at each branch are denoted by symbol "a". For example, at $k=3$, the corresponding sub-channels are labeled as "a", "b", "c", and "d" so that the channels can be represented by $k=3a$, $3b$, $3c$, and $3d$, respectively.

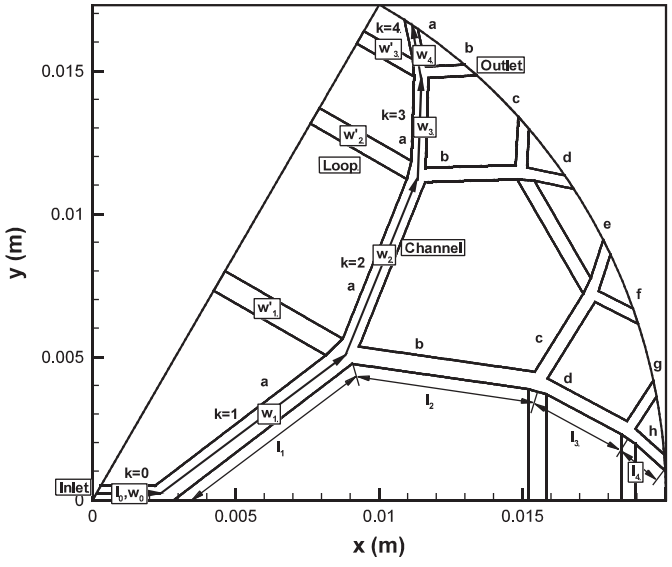

Fig. 2. Two-dimensional view of 1/6 part of tree-shaped microchannel nets ($n=2$, $m=4$).

Table 1
Dimensions of tree-shaped microchannel nets ($r=20$ mm).

	k	h_t(mm)	w_k (mm)	d_k (mm)	x_k (mm)	θ (°)	l_k (mm)	A (mm^2)
$m=1$	0	0.5	1	0.6667	4.28	120	4.28	97.91
	1	0.5	0.7937	0.6135	15.72	74.94	16.44	
$m=2$	0	0.5	1	0.6667	3.14	120	3.14	140.2
	1	0.5	0.7937	0.6135	9.64	38.85	10.18	
	2	0.5	0.63	0.5575	7.22	36.77	8.64	
$m=3$	0	0.5	1	0.6667	3.06	120	3.06	180.85
	1	0.5	0.7937	0.6135	7.76	40.6	8.32	
	2	0.5	0.63	0.5575	6.22	36.79	7.36	
	3	0.5	0.5	0.5	2.96	42.39	3.88	
$m=4$	0	0.5	1	0.6667	2.18	120	2.18	218.36
	1	0.5	0.7937	0.6135	8.04	37.5	8.4	
	2	0.5	0.63	0.5575	5.84	38.1	6.74	
	3	0.5	0.5	0.5	2.78	43.1	3.6	
	4	0.5	0.3968	0.4425	1.16	49.8	1.736	

As shown in Fig. 1, the bottom wall is subjected to a constant heat flux of q''_0. The height of the heat sink system h can be expressed as the sum of the height of heat sink is h_s, tree-shaped nets h_t and chip h_c, i.e., $h=h_s+h_t+h_c$. The channel is cooled by a single-phase fluid at T_0 which is forced into the channel by a specified mass flow ($\dot{m}$). The coolant is modeled as a Newtonian fluid with the temperature-dependent properties given in Table 2. And the properties of solid (silicon) are assumed constant at temperature $T=310$ K, as shown in Table 2.

Numerous investigations of single-phase gas and liquid flow and heat transfer in microchannel over the past decade have been reviewed by Rostami et al. [31,32] and Obot [33]. Based on examination of previous work, Obot [33] concluded that for scales of characteristic length larger than 10 μm, the Navier–Stokes equations are appropriate to describe the transport phenomena since there is no supporting evidence to suggest that the fluid flow in microchannels behaved differently from that in macro-scale channels. Lawal and Mujumdar [34] reviewed the laminar flow and heat transfer of viscous non-Newtonian fluids in ducts of various geometries such as circular pipes, parallel plates, rectangular and triangular ducts, etc. by numerically solving the Navier–Stokes and energy equations in three dimensions in conjunction with a constant heat flux boundary condition at the channel walls. The current numerical simulations were conducted using Fluent 6.3 which is a CFD code based on the finite volume method. A steady,

Table 2
Properties of liquid (water) and solid.

	Silicon ($T=310$ K)	Water ($p=1$ atm, 273.15 K $\le T \le$ 373.15 K)
Density ρ (kg/m^3)	2330	$914.56+1.30T-0.036T^2$
Thermal conductivity λ (W/m K)	125	$-0.794+7.628\times10^{-3}T-9.866\times10^{-6}T^2$
Specific heat capacity c_p (J/kg K)	700	$1089.03-58.15T+0.166T^2-1.55\times10^{-4}T^3$
Dynamic viscosity μ (Pa s)		$0.458-5.29\times10^{-3}T+2.30\times10^{-5}T^2-4.45\times10^{-8}T^3+3.24\times10^{-11}T^4$

incompressible and laminar flow is assumed. The governing equations for the steady-state conservation of mass, momentum and energy in Cartesian coordinates are as follows:

$$\frac{\partial V_i}{\partial x_i} = 0 \tag{3}$$

$$\rho\frac{\partial(V_i V_j)}{\partial x_i} = \frac{\partial}{\partial x_i}\left(\mu\frac{\partial V_j}{\partial x_i}\right) - \frac{\partial p}{\partial x_i} \tag{4}$$

$$\rho\frac{\partial(V_i c_p T)}{\partial x_i} = \frac{\partial}{\partial x_i}\left(\lambda\frac{\partial T}{\partial x_i}\right) \tag{5}$$

As shown in Figs. 1 and 2, the flow emanates from the center of the disc to the point at the perimeter of the disc. The mass flow inlet and pressure outlet are applied. The total mass flow is 3 g/s, which is distributed evenly into each channel at the zeroth-level. For example, if the disc has three channels at the center, then $\dot{m} = 1$ g/s is the mass flow rate under the inlet boundary condition of the computational domain. Note that the corresponding Reynolds number is around 200 at the inlet and typical Knudsen number is about 0.0015. The reference pressure (atmosphere pressure) is specified at the outlet. As compared to the outer heat sink and chip, channels are of smaller scales. To ensure accuracy of simulation in the channels and control the total number of grids, we need to use two-level grids with different size steps for the channels and the outer part. To connect the two parts, a conjugate interface between channels and outer walls was chosen. Along the top wall of the sink, a constant heat flux of $q_0'' = 10\ \mathrm{W/cm^2}$ is applied. Other walls are specified to be adiabatic.

Grid-independence of the final results was checked for each geometrical configuration by analysis of pressure distribution of four designs of the mesh with different grid densities. The comparison shows that the difference of pressure drop between the $12 \times 12 \times$ mod and $16 \times 16 \times$ mod is only 0.7%. Therefore, the final grid system used here is about $16 \times 16 \times$ mod (l_k/0.1 mm) for each channel segment. And for the outer domain, we use a size step of 0.2 mm for the x- and y-directions and 32 grids in the z-direction.

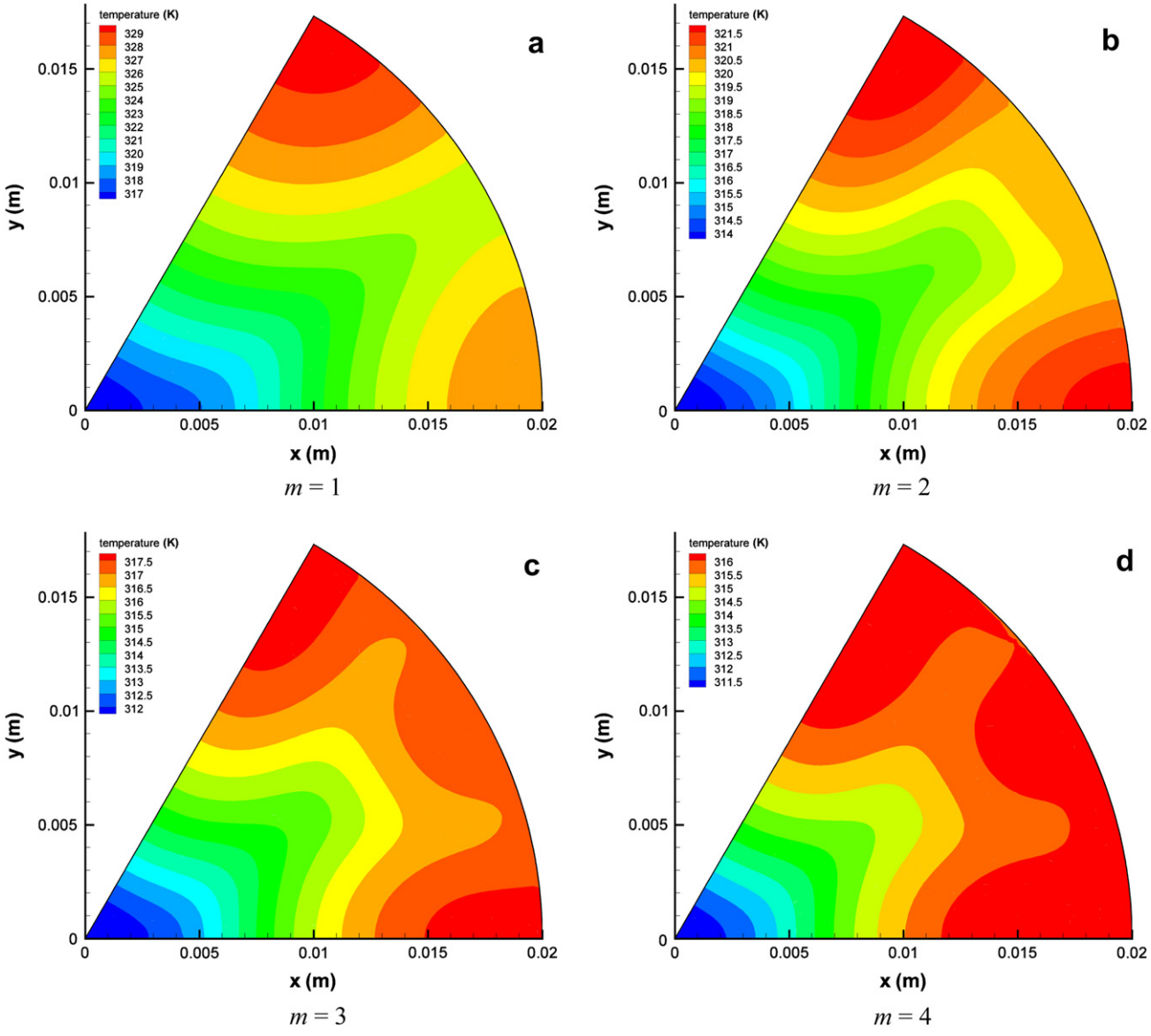

Fig. 3. Temperature contours over the bottom surface of chip ($z = -h_c$) for tree-shaped nets *without* loops.

Boundary layer mesh technique was used to control the mesh quality along the slim channel nets. Considering the different designs of geometries, the total number of grid nodes is arranged from 391,421 to 553,310 with increasing branch levels. For the full geometry study, the grids are relatively large, around 2,944,818. Since the cases were submitted to cluster, around 1 h is required for each case under 16 parallel nodes.

3. Results and discussions

The numerical results can be validated by comparison with analytical and numerical solutions from literature, as suggested by Senn and Poulikakos [35]. The numerical value of $f \times Re = 56.94$ of the straight parallel nets is in good agreement with the analytical solution given by Moody (or Darcy) as [36]

$$f \times Re = 24\left[1 - 192\pi^{-5}\sum_{n=1,3,\ldots}^{\infty} n^{-5}\tanh\left(\frac{n\pi}{2}\right)\right]^{-1} \cong 56.908 \tag{6}$$

We will focus on the influence of total branching level m in tree-shaped nets with/without loops and effect of loops with/without blockages. It is noted that for the cases without blockages or with

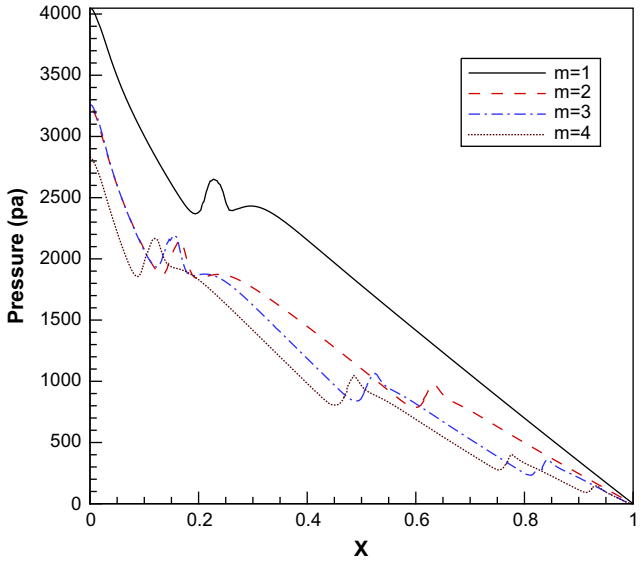

Fig. 5. Pressure distribution along one path of the tree-shaped nets *without* loops.

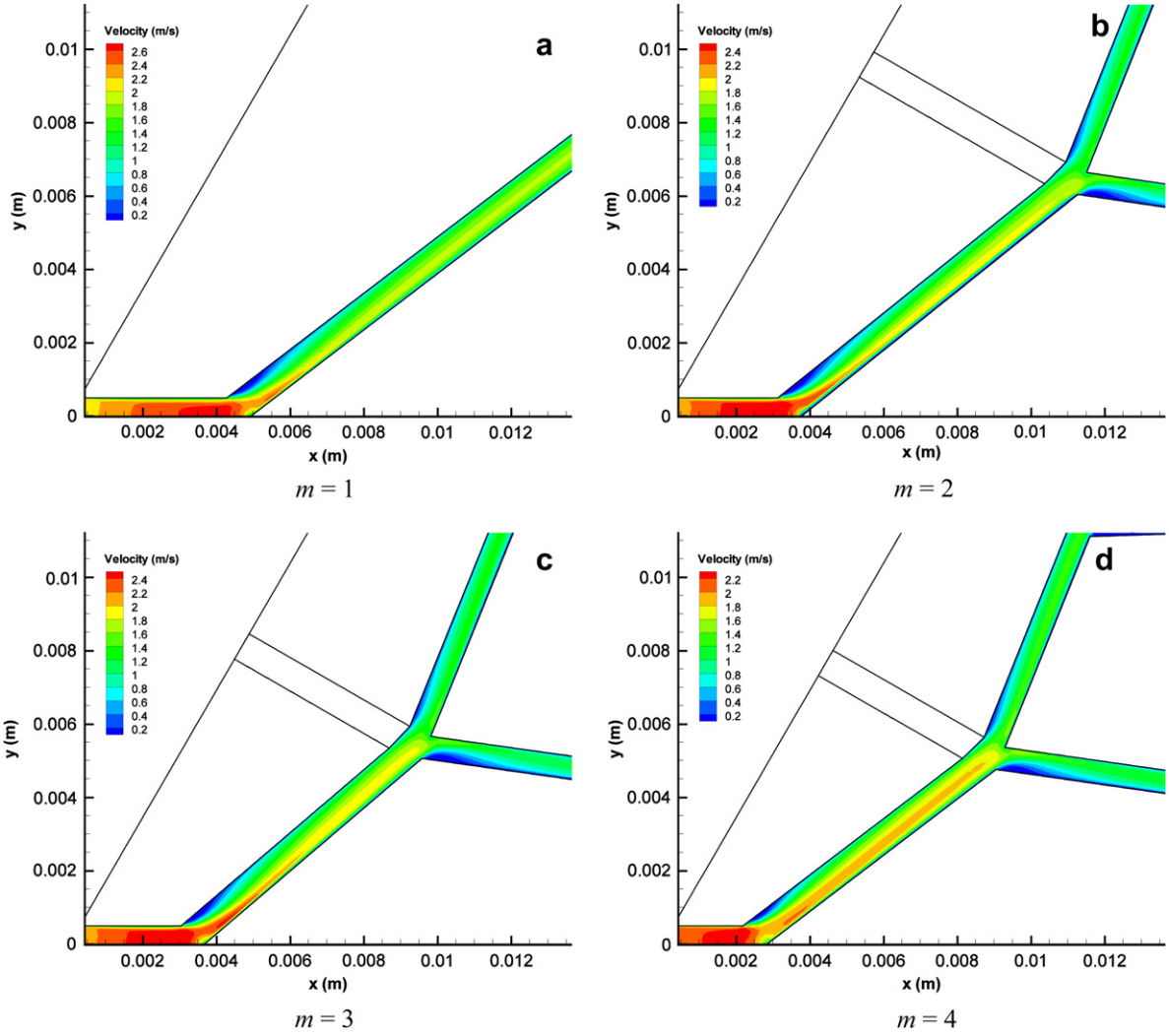

Fig. 4. Fluid flow velocity contours on the middle plane of the channels ($z = h_t/2$) for tree-shaped nets *without* loops.

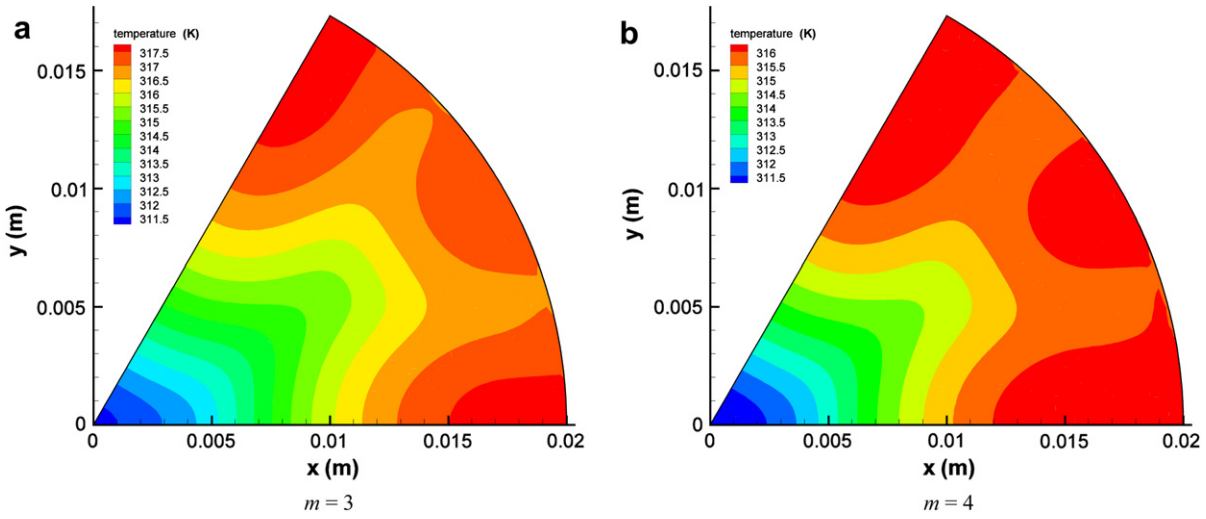

Fig. 6. Temperature contours over the bottom surface ($z = -h_c$) for tree-shaped nets *with* loops.

symmetrical blockages, considering symmetry in the net geometries, only 1/6 part of the full geometry was simulated, as shown in Fig. 2. But, in practice such symmetrical blockage will be seldom. Hence, to investigate the effect of loops in the non-symmetrical blockages (random blockages), full geometrical maps should be discussed.

3.1. *Effect of total branching level for tree-shaped nets without/with loops*

First, for the general tree-shaped flow networks without loops, Fig. 3 shows the computed temperature distribution on the bottom surface ($z = -h_c$) of the chip (refer to Fig. 1) for four nets: $m = 1, 2, 3$, and 4. As mentioned previously, considering the symmetrical distribution of the channel nets in the heat sink, only 1/6th part ($N = 3$) of the full geometry was simulated. From the figures it is observed that the maximum temperature difference between the highest and lowest ΔT_{max} is 11.5 K for $m = 1$, followed by 7.7 K for $m = 2$, 5.5 K for $m = 3$, and 4.5 K for $m = 4$. Since the maximum temperature difference represents the non-uniformity of the temperature distribution on the surface, it can be found that with an increase of number of branch levels, the temperature distribution is more uniform. Note that the large temperature gradient among the chip would result in thermal expansion of the materials and may cause failure of the system. Hence, uniformity of the system is an important condition to be achieved. Furthermore, if we plot ΔT_{max} versus total branching levels m, it is clearly shown that the improvement of temperature distribution is decreased with increasing m. This means that the high branching level channel net is not a good choice considering the increased complexity of geometry as compared to the limited improvement of temperature distribution.

Fig. 4 demonstrates the velocity distribution in the middle plane of the channel nets ($z = h_t/2$) for the four tree-shaped nets without loops. Only enlarged regions between $k = 1$ and $k = 2$ are displayed for clarification. As seen from the figures, the fluid flow is diverted at each bifurcation. Due to fluid inertia, the main stream is closer to the inner walls. Hence, there is a low velocity region with a vortex at the corner near the outer walls, as shown in the figures in blue. Also, the bifurcation point causes stagnation of the flow. Hence, the laminar boundary layer has to redevelop at each sub-channel, which results in recovery of the local pressure as spikes. Consequentially, the global pressure drop decreases as compared to parallel straight channels; this was already shown in the work of

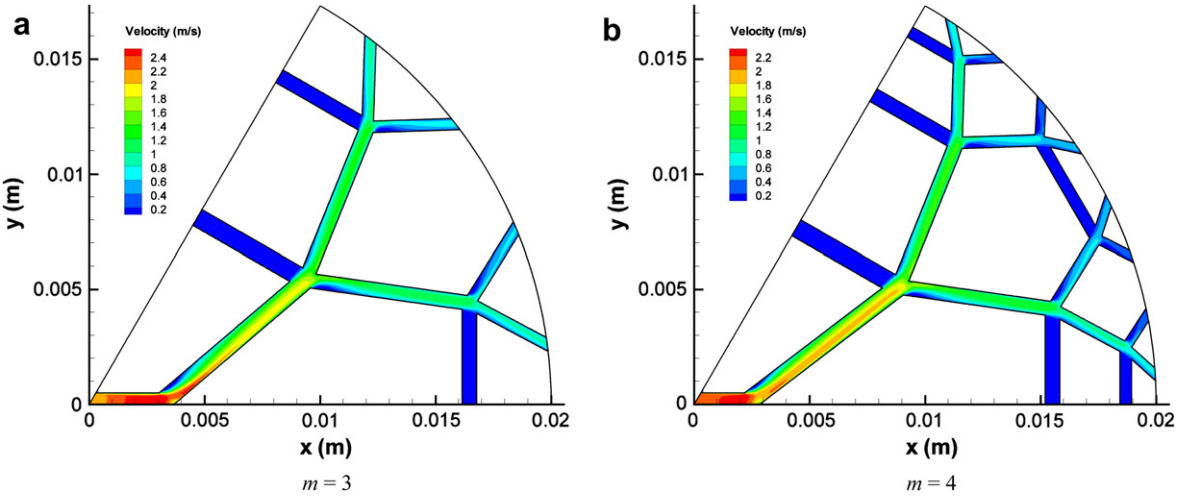

Fig. 7. Fluid flow velocity contours on the middle plane of the channels ($z = h_t/2$) for tree- shaped nets *with* loops.

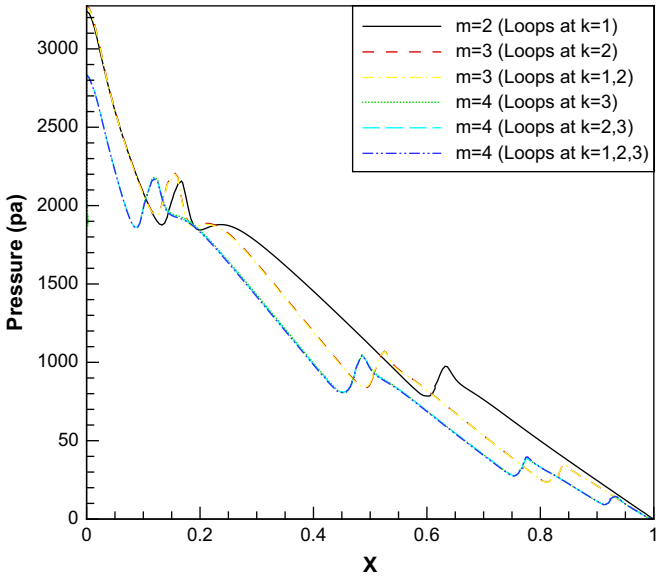

Fig. 8. Pressure distribution alone one path of the tree-shaped nets *with* loops.

Pence [30] and Wang et al. [10]. It is noted that the non-uniformity of the velocity distribution is not desirable in practice. Fortunately it can be decreased using streamlined bifurcations.

Fig. 5 shows the predicted pressure distribution along one path (as shown in a series of arrows in the channel nets in Fig. 2) of the tree-shaped nets without loops, where the dimensionless parameter $X = x/r$. In Fig. 5, as discussed previously, the redevelopment of the laminar boundary layer at each sub-channel results in spikes in the local static pressure distribution, which contributes to the overall decrease of the pressure drop as compared to straight channel nets. Furthermore, the total pressure drop decreases with increasing number of branch levels. It is easily explained since the increased branch levels would produce increased number of spikes in the local pressure.

What is the effect if the loops between the main channels are activated? Note that the loops are connected by channels between bifurcations of the same branch level, as shown in Fig. 1. Fig. 6 displays the temperature contours over the bottom chip surface ($z = -h_c$) for the two typical tree-shaped nets with activated loops: $m = 3$ and $m = 4$. As compared to the temperature distribution of nets without loops as shown in Fig. 3(c) and (d), it is found that the thermal patterns are nearly same for both cases. This means the effect of the activated loops on the heat transfer characteristics is insignificant. The maximum temperature (317.5 K and 316 K for $m = 3$ and $m = 4$, respectively) of the nets with loops is also seen to be the same as that of the tree-shaped channel net without loops. The reason for this observation can be checked from the velocity distribution over middle plane $z = h_t/2$, as shown in Fig. 7. It is observed that the loops do not involve any fluid flow. Only small expansion of the flow pattern occurs at the connections between the main channels and the loops. Symmetrical distribution of channels and loops causes stagnation of the fluid in the loops. Hence, inclusion of loops does not affect the fluid flow and heat transfer performance of the original tree-shaped nets, which is good news for the designers since they need not consider again the optimization of tree-shaped nets with loops. Instead, optimization of loops can be considered separately. Note that the main purpose of loops is to alleviate the deterioration during blockage of channels, which is discussed in a later section. Fig. 8 illustrates the pressure distribution along one typical path (noted by arrows in Fig. 2) of the tree-shaped nets with loops. The loops at different branch levels were activated one by one. However, as compared to Fig. 5, it is seen from the figure that the inclusion of any loops has neglected the effect on the pressure distribution for all the tree-shaped nets due to the symmetrical structure of the nets.

3.2. Effect of loops for tree-shaped nets with blockages

Due to the small diameters of the segments in a microchannel net, some of the sub-channels may become blocked in practice; this may be caused by particles in the working fluids or physical damage to the channel itself. It is important to deal with such possibilities in practice. Otherwise, the whole system may fail due to development of local hot spots. For the conventional parallel straight channel nets, blockage of any channel will cause stagnation of the flow in whole channel. Heat only can be carried away by the neighboring channels in such a case. Hence the temperature around the blocked channel is higher than that in other regions; this is not desirable. What we need to design for is to minimize the affected area and maintain global performance. With introduction of tree-shaped microchannel nets, this requirement can be met.

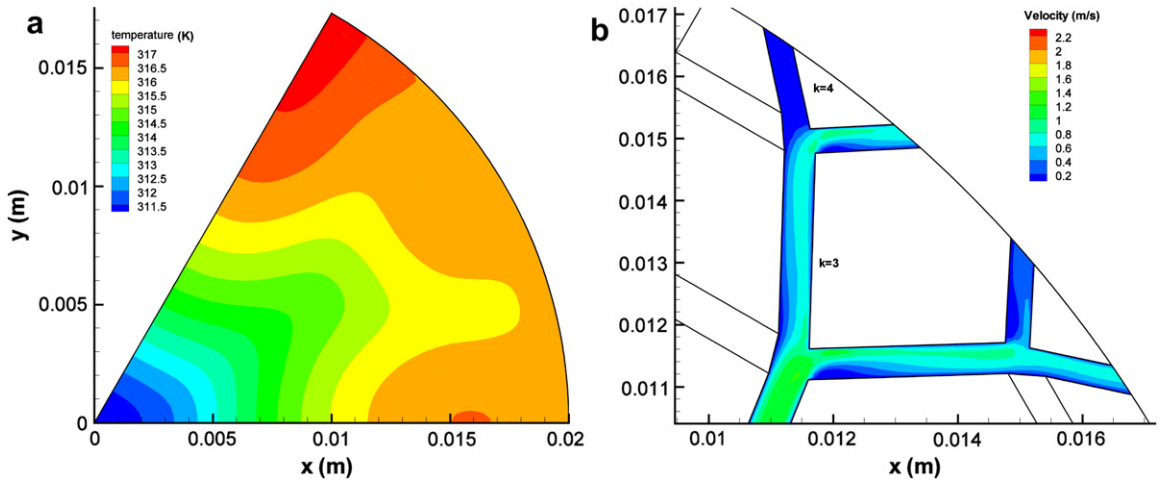

Fig. 9. (a) Temperature contours over the bottom surface ($z = -h_c$) and (b) fluid flow velocity contours on the middle plane of channels ($z = h_t/2$) for four-branching level tree-shaped nets without loops under blockage at outlet-4a.

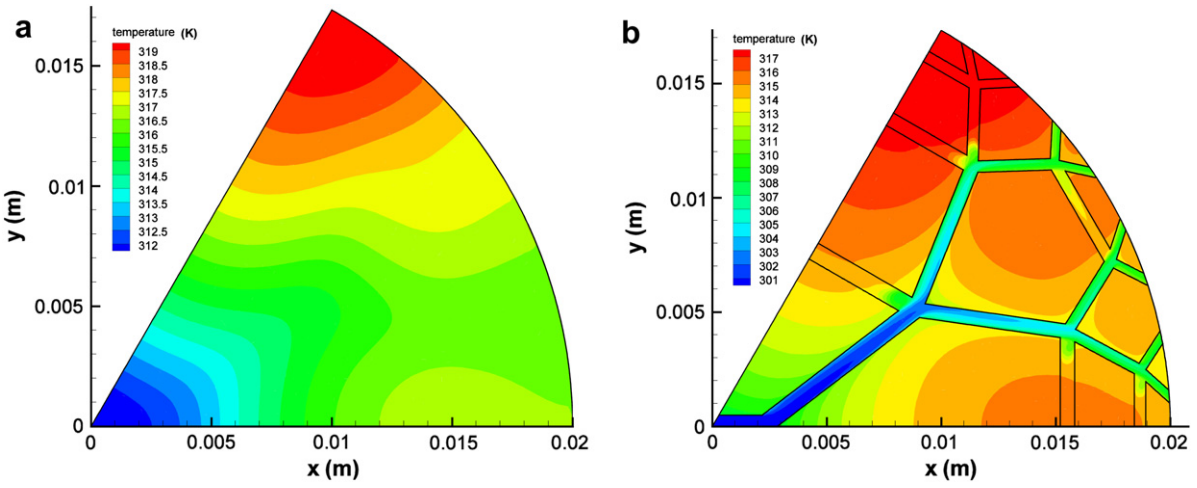

Fig. 10. (a) Temperature contours over the bottom surface ($z = -h_c$) for four-branching level tree-shaped nets without loops under blockage at outlet-4a and outlet-4b, (b) Temperature contours on the middle plane of channels ($z = h_t/2$) for four-branching level tree-shaped nets with loops under blockage at outlet-4a and outlet-4b.

Following previous studies, if one of the outlets (ka) is blocked physically, the maximum temperature difference ΔT_{max} increases from 4.5 K to 5.1 K for four-branching level channels without loops (Fig. 9(a)). The results indicate that the blockage of one outlet has only a minor effect on the thermal performance, which can be explained by the fluid flow in microchannels shown in Fig. 9(b). The blockage at outlet-4a causes stagnation of the fluid in channel 4a so that the fluid has to be diverted into the neighboring channel 4b. Due to the fixed width of the channel, the velocity in channel 4b increases slightly as compared to that in other channels at the same branching level. It is clear that the increased velocity would remove more heat from the blocked region. Thus, the tree-shaped channel net can avoid global failure of system. In particular, for the channel networks with higher branching levels, the effect is much smaller since the number of outlets is greater so that blockage of one outlet will affect only a smaller region.

To further investigate the effect of loops on the performance of tree-shaped nets, two outlets (outlet-4a and outlet-4b) are blocked physically in the next simulation. Fig. 10(a) shows the temperature distribution over the bottom chip surface ($z = -h_c$) for four-branching tree-shaped nets *without* loops, while Fig. 10(b) indicates temperature distribution on the middle plane of channels ($z = h_t/2$) for four-branching tree-shaped nets *with* loops. As compared to that of the single outlet blocked (Fig. 9), the effect of blockage on the temperature gradient is now more serious. The maximum temperature difference ΔT_{max} increases from 5.1 K to 7.1 K for tree-shaped nets without loops, although the thermal patterns are similar for both cases of blockage. Even with such serious blockages at outlets, the whole system still functions well considering the change of temperature gradient. Hence, the results demonstrate a robust performance of such tree-shaped channel networks. It is noted from Fig. 10(b) that inclusion of loops does not alleviate the problem caused by blockage. As compared to the cases without loops, the maximum temperature difference ΔT_{max} does not change much.

Due to the symmetry of the tree-shaped nets and heat sink systems, blockage at one outlet or two outlets in 1/6 part of channel networks means other five corresponding outlets are also blocked. That is the blockage of outlets is also symmetrical. Hence, the loops

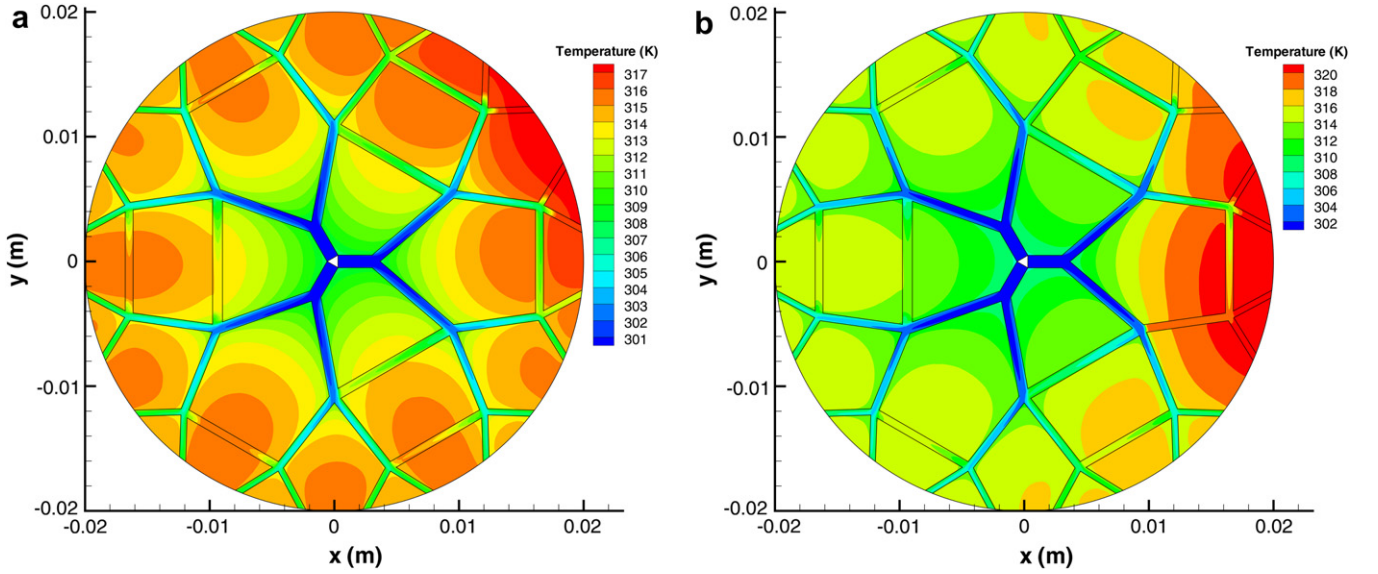

Fig. 11. Temperature contours on the middle plane of channels ($z = h_t/2$) for (a) three-branching level tree-shaped nets without loops under blockage at four outlets (3a–3d) and (b) three-branching level tree-shaped nets with loops under blockage at six outlets (3a–3f).

cannot be involved in the role of diversion of fluid from blocked channels. Although the loops are activated, the heat transfer characteristics are similar to those of cases without loops. Hence, to study the effect of blockage in tree-shaped nets with loops effectively, numerical simulation of full geometry must be carried out.

Considering the large number of needed grids (around 3 million), only one tree-shaped net ($m = 3$) was investigated here. Fig. 11(a) shows the temperature distribution over the middle plane of the channels ($z = h_t/2$) for the tree-shaped net ($m = 3$) without loops under blockages at outlet-3a–3d. As compared to the case without blockage, the maximum temperature difference ΔT_{max} increases from 14.1 K to 15.6 K. As compared to the cases without loops, the increase of $\Delta T_{max} = 17.9$ K for tree-shaped nets with loops is relatively smaller, even for serious blockage such as simultaneous blockage of six adjacent outlets (3a–3f) in Fig. 11(b), which is impossible in conventional parallel straight channel nets. Hence, tree-shaped nets with loops clearly show their superiority in cases involving non-symmetrical blockages. Other than the fact that the sub-channels can divert the fluid in blocked segments, the loops also can be activated due to the loss of global symmetry during partial blockages. Hence, both the sub-channels and loops work together to remove the heat from the blocked region. If the inner channels rather than the outlets are blocked, the inner loops would be activated to transport the fluid instead, which may cause more complex flow and thermal pattern, but the temperature gradient can still be maintained within acceptable level.

4. Concluding remarks

The flow and thermal performances of several tree-shaped nets without/with loops are investigated numerically. Results show that for nets without loops, increased branching level can decrease the temperature gradient and pressure drop over the system. For nets with loops, during normal working conditions (e.g. no blockage) or symmetrical blockages, the effect of loops on fluid flow and heat transfer characteristics is negligible. However, when the channel nets are blocked partially, the tree-shaped nets with loops perform significantly better than nets without loops, although the results of nets without loops are also acceptable. Since the inclusion of loops does not affect the performance of nets much during normal operation but increase the performance during blockage, such tree-shaped nets with loops maybe a good choice for design of electronic cooling systems of the future.

Acknowledgements

This work was jointly supported by National Natural Science Foundation of China through grant number 10572052 and China Scholarship Council Study Abroad Scholarship Program. Partial support by M3TC at National University of Singapore is also acknowledged.

References

[1] A. Bejan, Shape and Structure, from Engineering to Nature, Cambridge University Press, Cambridge, 2000.
[2] Y. Chen, P. Cheng, Heat transfer and pressure drop in fractal tree-like microchannel nets, Int. J. Heat Mass Transf. 45 (2002) 2643–2648.
[3] A.Y. Alharbi, D.V. Pence, R.N. Cullion, Fluid flow through microscale fractal-like branching channel networks, J. Fluids Eng. 125 (2003) 1051–1057.
[4] P. Xu, B. Yu, The scaling laws of transport properties for fractal-like tree networks, J. Appl. Phys. 100 (2006) 104906.
[5] X.Q. Wang, A.S. Mujumdar, C. Yap, Effect of bifurcation angle in tree-shaped microchannel networks, J. Appl. Phys. 102 (2007) 073530.
[6] A. Bejan, Constructal tree network for fluid flow between a finite-size volume and one source or sink, Rev. Gen. Therm. 36 (1997) 592–604.
[7] A. Bejan, N. Dan, Constructal trees of convective fins, J. Heat Transf. 121 (1999) 675–682.
[8] W. Wechsatol, S. Lorente, A. Bejan, Optimal tree-shaped networks for fluid flow in a disc-shaped body, Int. J. Heat Mass Transf. 45 (2002) 4911–4924.
[9] L. Gosselin, A. Bejan, Tree networks for minimal pumping power, Int. J. Therm. Sci. 44 (2005) 53–63.
[10] X.Q. Wang, A.S. Mujumdar, C. Yap, Numerical analysis of blockage and optimization of heat transfer performance of fractal-like microchannel nets, J. Electron. Packag. 128 (2006) 38–45.
[11] X.Q. Wang, C. Yap, A.S. Mujumdar, Laminar heat transfer in constructal microchannel networks with loops, J. Electron. Packag. 128 (2006) 273–280.
[12] A.M. Morega, A. Bejan, A constructal approach to the optimal design of photovoltaic cells, Int. J. Green Energy 2 (2005) 233–242.
[13] Y. Azoumah, P. Neveu, N. Mazet, Optimal design of thermochemical reactors based on constructal approach, AICHE J. 53 (2007) 1257–1266.
[14] A. Bejan, D. Gobin, Constructal theory of droplet impact geometry, Int. J. Heat Mass Transf. 49 (2006) 2412–2419.
[15] A.H. Reis, A.F. Miguel, A. Bejan, Constructal theory of particle agglomeration and design of air-cleaning devices, J. Phys. D: Appl. Phys. 39 (2006) 2311–2318.
[16] A.K. da Silva, L. Gosselin, Constructal peripheral cooling of a rectangular heat-generating area, J. Electron. Packag. 128 (2006) 432–440.
[17] K.M. Wang, S. Lorente, A. Bejan, Vascularized networks with two optimized channel sizes, J. Phys. D: Appl. Phys. 39 (2006) 3086–3096.
[18] K.M. Wang, S. Lorente, A. Bejan, Vascularization with grids of channels: multiple scales, loops and body shapes, J. Phys. D-Appl. Phys. 40 (2007) 4740–4749.
[19] A. Bejan, S. Lorente, Constructal theory and its relevance to green energy, Int. J. Green Energy 4 (2007) 105–117.
[20] A.H. Reis, A. Bejan, Constructal theory of global circulation and climate, Int. J. Heat Mass Transf. 49 (2006) 1857–1875.
[21] D.V. Pence, in: Proceedings of the International Conference on Heat Transfer and Transport Phenomena in Microscale, Canada and Begell House, New York, 2000.
[22] W. Wechsatol, S. Lorente, A. Bejan, Tree-shaped networks with loops, Int. J. Heat Mass Transf. 48 (2005) 573–583.
[23] L.A.O. Rocha, S. Lorente, A. Bejan, Conduction tree networks with loops for cooling a heat generating volume, Int. J. Heat Mass Transf. 49 (2006) 2626–2635.
[24] C.D. Murray, The physiological principle of minimum work. I. The vascular system and the cost of blood volume, Proc. Natl. Acad. Sci. USA 12 (1926) 207–214.
[25] T.F. Sherman, On connecting large vessels to small. The meaning of Murray's law, J. Gen. Physiol. 78 (1981) 431–453.
[26] G.B. West, J.H. Brown, B.J. Enquist, A general model for the origin of allometric scaling laws in biology, Science 276 (1997) 122–126.
[27] D.V. Pence, K.E. Enfield, Inherent benefits in microscale fractal-like devices for enhanced transport phenomena, in: M. Collins, C.A. Brebbia (Eds.), Design and Nature, WIT Press, Greece, 2004, pp. 317–328.
[28] A. Bejan, L.A.O. Rocha, S. Lorente, Thermodynamic optimization of geometry: T- and Y-shaped constructs of fluid streams, Int. J. Therm. Sci. 39 (2000) 949–960.
[29] C.D. Murray, The physiological principle of minimum work applied to the angle of branching of arteries, J. Gen. Physiol. 9 (1926) 835–841.
[30] D.V. Pence, Reduced pumping power and wall temperature in microchannel heat sinks with fractal-like branching channel networks, Microscale Thermophys. Eng. 6 (2002) 319–330.
[31] A.A. Rostami, N. Saniei, A.S. Mujumdar, Liquid flow and heat transfer in microchannels: a review, Heat Technol. 18 (2000) 59–68.
[32] A.A. Rostami, A.S. Mujumdar, N. Saniei, Flow and heat transfer for gas flowing in microchannels: a review, Heat Mass Transf. 38 (2002) 359–367.
[33] N.T. Obot, Toward a better understanding of friction and heat/mass transfer in microchannels – a literature review, Microscale Thermophys. Eng. 6 (2002) 155–173.
[34] A. Lawal, A.S. Mujumdar, Laminar duct flow and heat transfer to purely viscous non-Newtonian fluids, Adv. Transp. Processes 5 (1987) 352–444.
[35] S.M. Senn, D. Poulikakos, Laminar mixing, heat transfer and pressure drop in tree-like microchannel nets and their application for thermal management in polymer electrolyte fuel cells, J. Power Sources 130 (2004) 178–191.
[36] R.K. Shah, A.L. London, Laminar Flow Forced Convection in Ducts, Academic Press, New York, 1978.